Role of Individual Methionines in the Fibrillation of Methionine-Oxidized α-Synuclein†

Mark J. Hokenson, Vladimir N. Uversky,* John Goers,‡ Ghiam Yamin, Larissa A. Munishkina, and Anthony L. Fink*

Department of Chemistry and Biochemistry, University of California, Santa Cruz, California 95064

Received January 1, 2004; Revised Manuscript Received February 17, 2004

ABSTRACT: The aggregation of normally soluble α-synuclein in the dopaminergic neurons of the *substantia nigra* is a crucial step in the pathogenesis of Parkinson's disease. Oxidative stress is believed to be a contributing factor in this disorder. We have previously established that oxidation of all four methionine residues in α-synuclein (to the sulfoxide, MetO) inhibits fibrillation of this protein in vitro and that the MetO protein also inhibits fibrillation of unmodified α-synuclein. Here we show that the degree of inhibition of fibrillation by MetO α-synuclein is proportional to the number of oxidized methionines. This was accomplished be selectively converting Met residues into Leu, prior to Met oxidation. The results showed that with one oxidized Met the kinetics of fibrillation were comparable to those for the control (nonoxidized), and with increasing numbers of methionine sulfoxides the kinetics of fibrillation became progressively slower. Electron microscope images showed that the fibril morphology was similar for all species examined, although fewer fibrils were observed with the oxidized forms. The presence of zinc was shown to overcome the Met oxidation-induced inhibition. Interestingly, substitution of Met by Leu led to increased propensity for aggregation (soluble oligomers) but slower formation of fibrils.

α-Synuclein is a small (14 kDa), highly conserved presynaptic protein that is abundant in various regions of the brain (*1*, *2*). Structurally, purified α-synuclein belongs to the family of natively unfolded proteins (*3*, *4*) which have little or no ordered structure under physiological conditions due to a unique combination of low overall hydrophobicity and large net charge (*5*). Misfolding and deposition of α-synuclein have been implicated in the pathogenesis of Parkinson's disease (PD),[1] multiple system atrophy, and several other neurodegenerative disorders, known as synucleinopathies (*6*, *7*). Fibrillar α-synuclein is involved in the formation of LBs and LNs (*8*), specific filamentous inclusions present in cytosol of some surviving nigral neurons in PD brains (*9*, *10*). The mutations A53T and A30P in α-synuclein have been identified in autosomal dominantly inherited, early-onset PD (*11*, *12*). Recently, it has been shown that triplication of the α-synuclein gene causes autosomal dominant PD with an average age of onset of 34 years (*13*). Finally, the production of α-synuclein in transgenic mice (*14*) or in transgenic flies (*15*) leads to motor deficits and neuronal inclusions reminiscent of PD.

α-Synuclein is readily assembled into fibrils in vitro, with morphologies and staining characteristics similar to those extracted from disease-affected brain (*4*, *16*−*21*). Fibrillation occurs via a nucleation-dependent polymerization mechanism (*17*, *20*) with a critical initial structural transformation from the unfolded conformation to a partially folded species (*4*).

The formation of reactive oxygen species is a normal byproduct of metabolism in cells. Organisms have evolved complex mechanisms to minimize oxidative damage to proteins and other macromolecules, as well as repair systems to reverse some oxidative modifications, and disposal systems to remove damaged macromolecules, which are not repaired. Usually, ROS are rendered harmless by antioxidants, metal chelators, or enzymatic reduction. However, when the level of ROS exceeds some threshold, these defense mechanisms may fail, and the cell may suffer from oxidative stress. Oxidation-modified proteins have been shown to accumulate during normal aging (*22*−*26*), and oxidative injury has been implicated in the pathogenesis of several disorders involving protein aggregation, including Alzheimer's disease (*25*−*28*), PD (*29*−*31*), dementia with LBs (*32*), Huntington's disease (*33*), and amyotrophic lateral sclerosis (*34*).

All amino acids are susceptible to oxidation, although their susceptibilities vary greatly (*22*), with methionine being one of the most readily oxidized amino acid constituents of proteins (*35*). Methionine is easily oxidized to methionine sulfoxide, by 2-electron oxidations such as with H_2O_2 among many other biological oxidants (*35*). Because this modification can be repaired by methionine sulfoxide reductase which catalyzes the reduction of MetO back to methionine (*36*, *37*), it is assumed that oxidation of surface-exposed methionines

† This research was supported by Grant NS39985 from the National Institutes of Health.

* To whom correspondence should be addressed. A.L.F.: tel/fax, (831) 459-2744; e-mail, enzyme@cats.ucsc.edu. V.N.U.: tel, (831) 459-2915; fax, (831) 459-2935; e-mail, uversky@hydrogen.ucsc.edu.

‡ Present address: Department of Chemistry and Biochemistry, California Polytechnic State University, San Luis Obispo, CA 93407.

[1] Abbreviations: PD, Parkinson's disease; LB, Lewy body; LN, Lewy neurite; ROS, reactive oxygen species; MetO, methionine sulfoxide; CD, circular dichroism; UV, ultraviolet; FTIR, Fourier transform infrared; SEC, size exclusion chromatography; EM, electron microscopy; ThT, thioflavin T; WT, wild type.

10.1021/bi049979h CCC: $27.50
Published on Web 03/26/2004

may protect other functionally essential residues from oxidative damage (*38*).

The cause of PD is unknown, but considerable evidence suggests a multifactorial etiology involving genetic and environmental factors (*39*, *40*). Oxidative injury has been assumed to be another causative agent in the pathogenesis of PD (*29*−*31*, *41*). The accumulation of nitrated α-synuclein (via oxidation by peroxynitrite) has been demonstrated in LBs (*29*, *42*, *43*). Formation of another product of tyrosine oxidation, dityrosine, has been detected in vitro during experiments on the aggregation of α-synuclein in the presence of copper and H_2O_2 (*44*) or catecholamines (*45*). We have recently established that all four methionines in α-synuclein, Met1, Met5, Met116, and Met127, are readily oxidized in vitro by low concentrations of H_2O_2, leading to effective inhibition of α-synuclein fibrillation (*46*).

In this report we analyze the structural and fibrillation properties of a series of α-synuclein mutants, whose Met residues were replaced by Leu. We show that the degree of inhibition of MetO α-synuclein fibrillation is proportional to the number of oxidized methionines.

MATERIALS AND METHODS

Materials. Aminopeptidase from *Aeromonas proteolitica* (EC 3.4.11.10, lot 22K4142) was purchased from Sigma (St. Louis, MO). Thioflavin T was obtained from Sigma (St. Louis, MO). All other chemicals were of analytical grade from Fisher Chemicals or VWR Scientific.

Mutagenesis and Expression of Human α-Synuclein. Wild-type and mutant human α-synucleins were expressed in an *Escherichia coli* BL21(DE3) cell line transfected with pRK172/α-synuclein plasmid. The M5L mutant was prepared with polymerase chain reaction amplification of wild-type α-synuclein pRK172/α-synuclein plasmid (*46*) by using a mutated 5′ primer designed to insert a leucine for methionine. All remaining mutants (M116L, M127L, M5L/M116L, M5L/M127L, M5L/M116L/M127L) were constructed using the QuikChange method (Stratagene, La Jolla, CA). Briefly, forward and reverse mutagenic primer pairs were designed with single nucleotide changes converting selected methionine into leucine codons. The mutagenic primer pairs were used to amplify the pRK172/α-synuclein plasmid which was used to transfect a BL21(DE3) cell line. Mutated α-synuclein genes in the plasmid were verified by DNA sequence analysis, and the cell line was then used for expression of protein (*46*). Multiple M to L mutants (e.g., M5L + M127L) were constructed from additional rounds of QuikChange mutational cloning of single or double mutants. The molecular masses of all mutant α-synucleins were verified by electrospray mass spectrometry.

Purification of α-Synuclein and Sample Preparation. Expression and purification of human recombinant α-synuclein and its mutants from *E. coli* were performed as previously described (*46*). After the purification, protein solutions were dialyzed four times against deionized H_2O at 4 °C, lyophilized, and stored at −80 °C.

Samples were prepared by dissolving lyophilized proteins in sterile H_2O/NaOH (pH 10.9) for 20 min on ice, followed by neutralizing with an appropriate buffer (see below). These solutions were either centrifuged at 14000 rpm for 10 min at 4 °C or ultracentrifuged at 100000 rpm for 10 min using a Beckman Airfuge to pellet any insoluble material. Protein concentrations were determined spectrophotometrically using an extinction coefficient $\epsilon_{276nm} = 0.401$ mg/mL.

Digestion with Aminopeptidase Enzyme. Ten units of aminopeptidase was added to 1 mL of approximately 10 mg/mL α-synuclein solution in 10 mM HEPES (pH 8.0) and incubated for 2.5 h at 37 °C. Digestion reactions with the enzyme were quenched with excess EDTA (to a final concentration of 60 mM) for 15 min at room temperature.

Separating α-synuclein from aminopeptidase, which is relatively similar in size (29500 Da) to natively unfolded α-synuclein, required the samples to be adjusted to 6 M Gdn·HCl in 10 mM HEPES (pH 8.0) for 15 min at 4 °C. This effectively unfolded the aminopeptidase, enabling it to be separated from natively unfolded α-synuclein by centrifugation at 3000 rpm for 2−2.5 h at 4 °C with a 100000 molecular weight cutoff Centricon (Amicon). Mass spectrometry demonstrated that only the N-terminal Met had been removed. The filtrate containing the truncated α-synuclein was dialyzed four times against deionized H_2O at 4 °C to remove excess Gdn·HCl.

Oxidation of α-Synuclein with Hydrogen Peroxide. Solutions of mutant and wild-type α-synuclein in 25 mM Tris-HCl and 100 mM NaCl (pH 7.6) were oxidized according to ref *46* by incubating protein solutions with 2−3% H_2O_2 for 20 min at 4 °C. Nonreacted peroxide was removed by ultrafiltration [with a 10000 MW cutoff Microcon or Centricon (Amicon)] at 7500 rpm for 2−2.5 h at 4 °C. That the only effect of the oxidation was conversion of all the methionines to the corresponding sulfoxides was confirmed with ESI mass spectrometry (MicroMass Quattro II).

Fluorescence Measurements. Fluorescence measurements were performed in semimicro quartz cuvettes (Hellma) with a 1 cm excitation light path using a FluoroMax-2 spectrofluorometer from Instruments S.A., Inc., Jobin Yvon-Spex. The light source was a 150 W xenon lamp. All data were processed using DataMax/GRAMS software.

Static Light Scattering. Static light scattering measurements were performed in semimicro quartz cuvettes (Hellma) with a 1 cm excitation light path using a FluoroMax-3 spectrofluorometer from Instruments S.A., Inc., Jobin Yvon-Spex. The light source was a 150 W xenon lamp. Scattering profiles were recorded with both excitation and emission at 350 nm. All data were processed using DataMax/GRAMS software.

Size Exclusion Chromatography (SEC). Association states of WT and mutated α-synucleins were estimated by gel filtration. SEC was performed on a TSK-GEL G2000SW_{XL} size exclusion column (7.8 mm i.d. × 30 cm) using a Waters 2695 separation module with a Waters 996 photodiode array (PDA) detector, and data were collected and analyzed by Millenium 32 software. Protein (∼0.1 mg/mL) was loaded onto the column, and the elution was carried out isocratically at a flow rate of 0.4 mL/min and monitored by the absorbance at 280 nm. Prior to measurement, solutions were filtered with a 0.1 μm Whatman Anodisc-13 filter. All measurements were made at 25 °C.

Circular Dichroism Spectroscopy. Far-UV CD spectra of 1.0 mg/mL wild-type and mutant α-synuclein were measured with an Aviv model 60DS spectrophotometer (Lakewood, NJ). Samples were analyzed in a 0.1 mm path length cell at 22 °C with a 3 s averaging time, a bandwidth of 1.5 nm,

and a step size of 1.0 nm. An average of four scans was obtained for each sample, and a spectrum of the buffer was subtracted to yield the final spectra.

Fourier Transform Infrared Spectroscopy. Spectra were collected with a ThermoNicolet Nexus 670 FTIR spectrometer equipped with a MCT detector and an ATR apparatus (SMART ARK) containing a 45° ZnSe IRE. Hydrated thin films of the samples were prepared and analyzed according to ref *47*. A total of 256 interferograms at 2 cm^{-1} resolution were taken for each sample.

Fibril Formation Assay. Assay solutions contained 15 μM ThT and α-synuclein at a concentration of 35 μM (0.5 mg/mL) in 20 mM Tris-HCl, 0.1 M NaCl, pH 7.5. A volume of 100 μL of the mixture was pipetted into a well of a 96-well plate (white plastic, clear bottom). The measurements were performed in the presence or absence of a Teflon bead ($^1/_8$ in. diameter; McMaster-Carr, Los Angeles, CA). Each sample was run in triplicate or quadruplicate. The plate was loaded into a fluorescence plate reader (Fluoroskan Ascent) and incubated at 37 °C with shaking at 600 rpm with a shaking diameter of 2 mm. The fluorescence was measured at 30 min intervals with excitation at 450 nm and emission at 485 nm. The results of these measurements were plotted as a function of ThT fluorescence intensity versus time and fitted by a sigmoidal curve as described in ref *48* by the following equation using SigmaPlot:

$$Y = y_i + m_i x + \frac{y_f + m_f x}{1 + e^{-[(x - x_o)/\tau]}}$$

where Y is the fluorescence intensity, x is time, and x_o is the time to 50% of maximal fluorescence. Thus, the apparent rate constant, k_{app}, for the growth of fibrils is given by $1/\tau$ (with τ being the elongation time), and the lag time (or nucleation time) is taken as $x_o - 2\tau$.

Electron Microscopy. Transmission electron micrographs were collected using a JEOL JEM-100B microscope operating with an accelerating voltage of 80 kV. Typical nominal magnifications were 75000×. Samples were deposited on Formvar-coated 300 mesh copper grids and negatively stained with 1% aqueous uranyl acetate.

RESULTS

We investigated the effects of the Met to Leu substitutions on both the nonoxidized and oxidized forms of the protein. Both characterization of the biophysical properties of the proteins and their tendencies to associate and aggregate to form fibrils were studied.

Production and in Vitro Oxidation of α-Synuclein and Its Mutants. There are four methionines in human α-synuclein, Met1, Met5, Met116, and Met127, which are readily oxidized in vitro in the presence of H_2O_2, leading to the effective inhibition of α-synuclein fibrillation (*46*). To understand the contribution of individual methionines to the conformational and aggregation behavior of human α-synuclein, we created a series of mutants containing methionine to leucine substitutions. This series includes three single mutants, M5L, M116L, M127L, which contain three Met residues; two double mutants, M5L/M127L and M116/M127, containing two Mets; a triple mutant, M5L/M116L/M127, which contains a single Met, and a triple mutant M116L/M127L, in which Met1 was removed by aminopeptidase, also containing a single Met; and a quadruple mutant, M5L/M116L/M127, in which Met1 was removed by aminopeptidase and contained no Met residues. Results of MS analysis of WT α-synuclein and the series of Met mutants prior to their oxidation are summarized in Table 1. In all the cases, MS revealed one species, whose molecular mass coincided with that expected for the particular α-synuclein mutant. The conditions used for the in vitro oxidation of the α-synucleins result in oxidation of all methionines present in a given protein (Table 1). This is evidenced by the MS peak corresponding to the mass of a given α-synuclein variant plus the corresponding number of oxygens (e.g., for wild-type protein, 14460 Da + 4 × 16 Da = 14524 Da; for a double mutant, 14423 Da + 2 × 16 Da = 14455 Da, etc.; see Table 1).

Table 1: Predicted and Measured Molecular Masses of Nonoxidized and Methionine-Oxidized α-Synucleins Analyzed in This Study

	mass		oxidized mass	
protein	expected	observed	expected	observed
4 methionines				
wild type	14460	14459 ± 2	14524	14524 ± 2
3 methionines				
M5L	14441	14441 ± 2	14489	14489 ± 2
M116L	14441	14441 ± 2	14489	14490 ± 2
M127L	14441	14442 ± 2	14489	14491 ± 2
2 methionines				
M5L/M127L	14423	14443 ± 2	14455	14455 ± 2
M116L/M127L	14423	14422 ± 2	14455	14455 ± 2
1 methionine				
M5L/M116L/M127L	14405	14406 ± 2	14421	14422 ± 2
M116L/M127L/(Met1)	14292	14292 ± 2	14308	14309 ± 2
no methionines				
M5L/M116L/M127L/(Met1)	14274	14273 ± 2	14274	14274 ± 2

Substitution of Leu for Met Has Little Effect on the Secondary Structure of α-Synuclein As Determined by Circular Dichroism. Figure 1A represents a set of far-UV CD spectra measured for WT, M5L, M116L, M127L, M5L/M127L, M116/M127, M116L/M127L/(Met1), M5L/M116L/M127, and M5L/M116L/M127/(Met1) α-synucleins, where (Met1) indicates Met1 is absent. The figure shows that the WT protein and the mutants with single or double mutations, M5L, M116L, M127L, M5L/M127L, M116/M127, and M116L/M127L/(Met1), have almost indistinguishable far-UV CD spectra. These spectra show the characteristic minima in the vicinity of 196 nm and the absence of bands around 210−230 nm, typical of an unfolded protein. This means that substitution of one or two leucines for methionines does not affect the structure of natively unfolded α-synuclein. On the other hand, substitution of three Met residues by Leu residues leads to small but reproducible changes in the spectra. Figure 1A shows that a decrease in the minimum at 196 nm for M5L/M116L/M127 and M5L/M116L/M127/(Met1) α-synucleins is accompanied by an increase in negative intensity around 222 nm, reflecting a small amount of mutation-induced formation of secondary structure.

Substitution of Leu for Met Leads to an Increased Propensity for Self-Association As Determined by FTIR. FTIR offers an alternative approach to analyze secondary structure in proteins. Experiments with low protein concen-

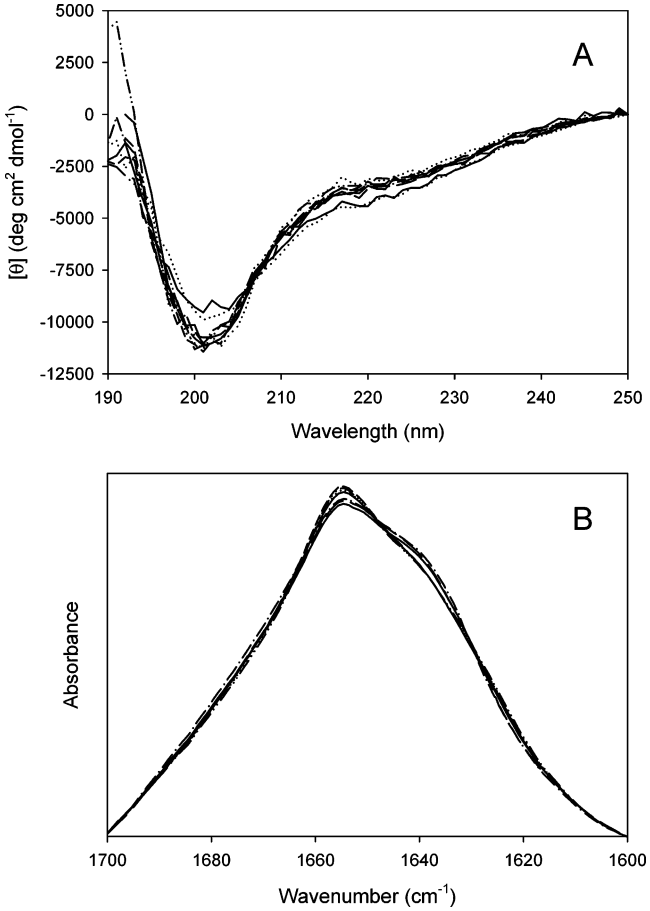

FIGURE 1: Secondary structure analysis of nonoxidized WT α-synuclein and its mutants with different Met → Leu substitutions. Far-UV CD (A) and FTIR spectra of the amide I region (B) were measured at pH 7.5. Line codes: WT (solid), M5L (dotted), M116L (short dashes), M127L (dash-dot-dot), M5L/M127L (long dashes), M116L/M127L (dash-dot), M116L/M127L/(Met1) (medium dashes), M5L/M116L/M127L (solid gray), and M5L/M116L/M127L/(Met1) (dotted gray), where (Met1) means that Met1 was absent (see text). For far-UV CD measurements the cell path length was 0.1 mm. Measurements were carried out at 23 °C. The protein concentration was 0.5 mg/mL.

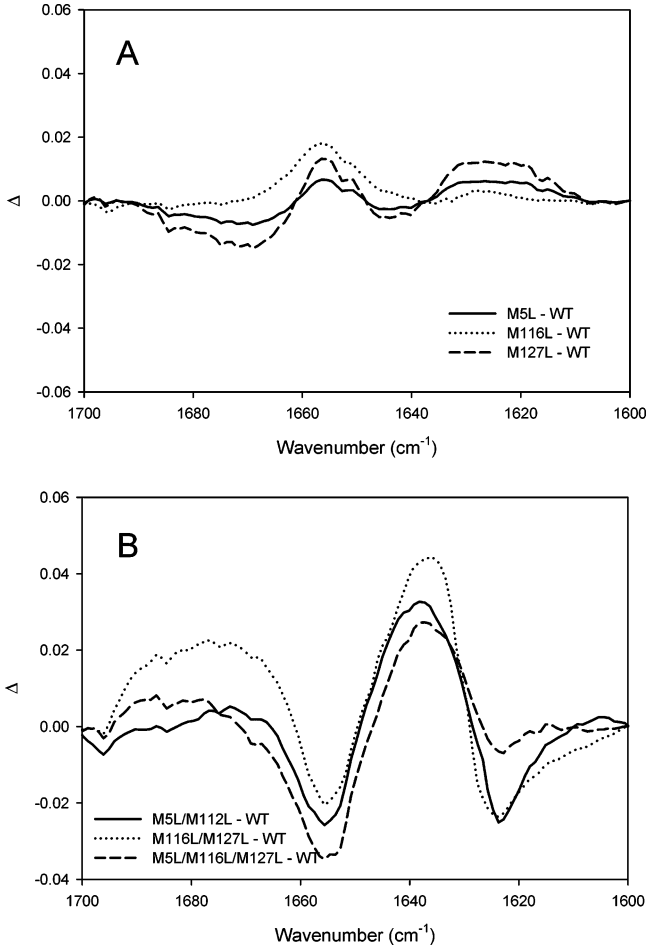

FIGURE 2: Met → Leu substitution-induced changes in α-synuclein secondary structure as detected by difference FTIR spectra. Difference spectra were calculated for single (A) and multiple mutants (B). In all cases the spectrum of WT α-synuclein has been subtracted from the spectrum of the corresponding mutant. Thus the difference spectra report the excess (positive values) or deficit of a particular structure (negative values) in the mutant as compared to the WT protein. Line codes: (A) M5L − WT (solid), M116L − WT (dotted), and M127L − WT (dashed); (B) M5L/M127 − WT (solid), M116L/M127L − WT (dotted), and M5L/M116L/M127L − WT (dashed).

trations are usually performed using attenuated total reflectance FTIR and hydrated thin films of the sample (*47*). There is a major methodological difference between CD and thin-film FTIR: the far-UV CD measurements are performed in dilute protein solutions (0.2 mg/mL), whereas the hydrated thin-film samples analyzed by FTIR have much higher concentrations (>1 mg/mL). It has been shown that the combined CD and FTIR analysis is able to discriminate proteins on the basis of their propensities to aggregate (*49*−*51*). Figure 1B represents the FTIR (amide I region) spectra measured for WT α-synuclein and the Met/Leu mutants at pH 7.5. The FTIR spectra of WT α-synuclein and single mutants are typical of a substantially unfolded polypeptide chain, whereas the spectra of M5L/M116L, M116L/M127, and M5L/M116L/M127 show small changes. The most evident change is the decrease of the band in the vicinity of 1655 cm^{-1}, which corresponds to disordered conformation, accompanied by the appearance of a new band in the vicinity of 1636 cm^{-1}, which corresponds to β-sheet. These observations are further illustrated in Figure 2, which represents the difference FTIR spectra. Figure 2B clearly shows that the depletion in signal in the vicinity of 1655 cm^{-1} occurs simultaneously with the rise of the signal around 1636 cm^{-1}. This means that the double and triple mutants of α-synuclein contain increased amounts of β-structure, probably due to association at the higher protein concentrations used in the FTIR experiments. This would indicate that the Leu-containing variants of α-synuclein had a greater propensity to associate than the wild type.

Deconvolution (FSD and second derivative) of the FTIR spectra, followed by curve fitting, permitted quantitation of the differences in the secondary structure between WT and mutant α-synucleins (not shown). These results revealed that the β-sheet content of the α-synucleins increases in the following order: WT < M5L = M116L = M127L < M5L/M127L = M116/M127 = M5L/M116L/M127.

Fluorescence Anisotropy, Static Light Scattering, and SEC Analyses Confirm the Increased Propensity of Leu Mutants To Associate. To validate the mutation-induced increase in the propensity of α-synuclein to associate, fluorescence anisotropy and static light scattering of the mutants were compared with those of WT. The data indicate that the anisotropy increases in the following order: WT (0.0580 ±

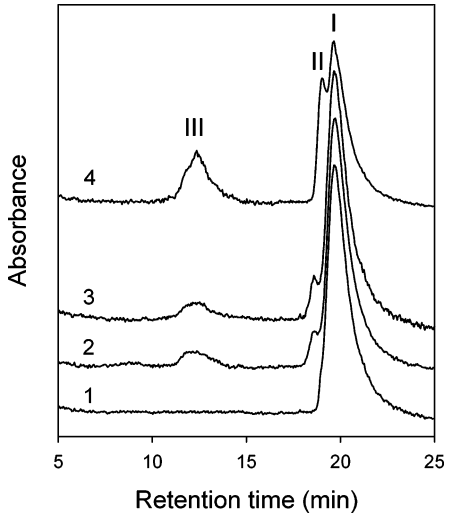

FIGURE 3: SEC analysis of the association state of WT α-synuclein (1) and its Met → Leu mutants: M5L (2), M115L (3), and M5L/M116L/M127L (4). Numbers above peaks correspond to monomer (I), dimer (II), and higher oligomer (III). SEC was performed on a TSK-GEL G2000SW$_{XL}$ size exclusion column. Proteins (~0.1 mg/mL) were loaded onto the column, and the elution was carried at a flow rate of 0.4 mL/min and monitored by the absorbance at 280 nm. All measurements were carried out at 25 °C.

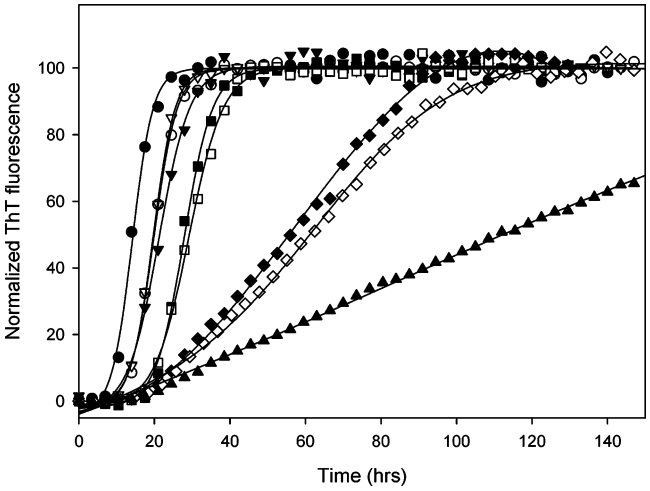

FIGURE 4: Kinetics of fibrillation of nonoxidized α-synucleins monitored by thioflavin T fluorescence. Measurements were performed at 37 °C and pH 7.5 in 20 mM sodium phosphate buffer containing 100 mM NaCl. Excitation was at 450 nm and emission at 482 nm. Symbols: WT (black circle), M5L (open circle), M116L (reversed black triangle), M127L (reversed open triangle), M5L/M127 (black square), M116L/M127 (open square), M5L/M116L/M127 (black diamond), M116L/M127/(Met1) (open diamond), and M5L/M116L/M127/(Met1) (black triangle).

0.0039) < M5L (0.0785 ± 0.0042) ≈ M116L (0.0763 ± 0.0045) < M116L/M127L (0.0962 ± 0.0083) < M5L/M116L/M127L (0.1188 ± 0.0103). Similarly, the magnitude of static light scattering increased in the solutions of the mutant α-synucleins in comparison with WT protein and generally followed the same trend, namely, WT (35000 ± 3000) < M5L (52000 ± 3000) ≈ M116L (54000 ± 3000) < M116L/M127L (71000 ± 5000) < M5L/M116L/M127L (115000 ± 5000). The changes in fluorescence anisotropy and static light scattering are attributed to the mutation-induced formation of soluble oligomers. Since these experiments were carried out without incubation, the results reflect the intrinsically increased propensity for association in the variants with the increased amount of Leu residues.

This was further confirmed by the size exclusion chromatography analysis of α-synuclein and its Met → Leu mutants. Figure 3 compares the elution profiles corresponding to the WT and mutated forms of α-synuclein. WT α-synuclein elutes as a single peak, whose elution volume corresponds to a monomeric protein. In contrast, mutated α-synucleins appear as mixtures of at least three different species, monomers, dimers, and higher oligomers. The relative populations of dimers and higher oligomers increase proportionally to the number of methionines substituted, replaced by leucines.

Overall, the data presented above show that Met → Leu substitutions do not have significant effects on the natively unfolded conformation of α-synuclein. However, the introduction of the more hydrophobic leucine residues increased the propensity for self-association. This effect was cumulative, as the α-synucleins form the following series in respect to their tendency to oligomerize: WT < single mutants < double mutants < triple mutants.

Effect of Met → Leu Substitutions on Fibrillation of Human α-Synuclein. Thioflavin T (ThT) is a fluorescent dye that interacts relatively specifically with amyloid fibrils, leading to an increase in the fluorescence intensity in the vicinity of 480 nm (*52*−*54*). Figure 4 compares the kinetics of fibrillation of the different variants of α-synuclein monitored by ThT fluorescence. Interestingly, all of the mutants studied formed fibrils more slowly than WT α-synuclein (see also kinetic parameters summarized in Table 2). Figure 4 and Table 2 show that the effect of the Met → Leu substitutions is to slow α-synuclein fibrillation in a cumulative manner. According to their rates of fibrillation, the α-synucleins can be arranged in the following order (from faster to slower rates of fibrillation): WT > M5L ≈ M116L ≈ M127L >M5L/M116L ≈ M116/M127 > M116L/M127L/(Met1) ≈ M5L/M116L/M127 > M5L/M116L/M127/(Met1). In other words, more Met residues correlated with faster fibrillation. The decrease in rate of fibrillation, induced by the Met → Leu substitutions, also correlates with the increased propensity of the mutated α-synucleins to oligomerize (self-associate).

Effect of Methionine Oxidation on the Secondary Structure of Human α-Synuclein and Its Mutants. The far-UV CD spectra of oxidized WT and Met mutants of α-synucleins are shown in Figure 5A, and the corresponding FTIR (amide I region) spectra are shown in Figure 5B. The far-UV CD spectra of MetO-α-synucleins measured at pH 7.5 are very similar to the spectra of the corresponding nonoxidized proteins. However, more detailed analysis of the spectra measured for WT and single and double mutants shows a slightly increased degree of disorder in comparison with the corresponding nonoxidized proteins. This was manifested by a small increase in negative ellipticity in the vicinity of 196 nm and somewhat lower intensity in the vicinity of 222 nm. This assumption was further confirmed by the analysis of spectral changes in the form of difference spectra. Figure 6A shows that the shape of the far-UV circular dichroism difference spectra (calculated for each protein as the difference between spectra of its nonoxidized and oxidized forms) corresponds to a change in β-structure, with a typical broad minimum in the vicinity of 220 nm and an intersection point

Table 2: Kinetic Parameters for the Fibrillation of Nonmodified and Methionine-Oxidized α-Synucleins

	nonoxidized			oxidized		
protein	$t_{1/2}$ (h)	lag time (h)	(elongation rate)$^{-1}$ (h)	$t_{1/2}$ (h)	lag time (h)	(elongation rate)$^{-1}$ (h)
WT	14.19 ± 0.07	8.65 ± 0.07	2.77 ± 0.06	ND[a]	ND	ND
M5L	19.82 ± 0.06	13.62 ± 0.07	3.10 ± 0.05	128.7 ± 0.9	76.9 ± 0.9	25.9 ± 0.5
M116L	21.23 ± 0.11	13.01 ± 0.11	4.11 ± 0.09	136.3 ± 1.5	90.3 ± 1.5	23.0 ± 0.5
M127L	19.71 ± 0.03	13.85 ± 0.03	2.93 ± 0.03	141.5 ± 0.9	93.3 ± 0.9	24.1 ± 0.5
M5L/M127L	27.90 ± 0.07	20.36 ± 0.07	3.77 ± 0.06	69.9 ± 0.2	41.1 ± 0.2	14.4 ± 0.2
M116L/M127L	29.13 ± 0.08	19.97 ± 0.08	4.58 ± 0.07	74.2 ± 0.2	41.8 ± 0.2	16.2 ± 0.21
M5L/M116L/M127L	55.64 ± 0.30	22.8 ± 0.3	16.40 ± 0.26	78.1 ± 0.3	28.1 ± 0.3	25.0 ± 0.3
M116L/M127L/(Met1)	56.45 ± 0.26	22.79 ± 0.26	16.83 ± 0.21	89.6 ± 0.7	28.2 ± 0.7	30.7 ± 0.6
M5L/M116L/M127L/(Met1)	83.8 ± 1.6	~20[b]	91.5 ± 1.8	76.2 ± 4.2	~20[b]	104.5 ± 5.2

[a] ND = not determined. [b]Values are estimated from the visual analysis of the corresponding kinetic curves.

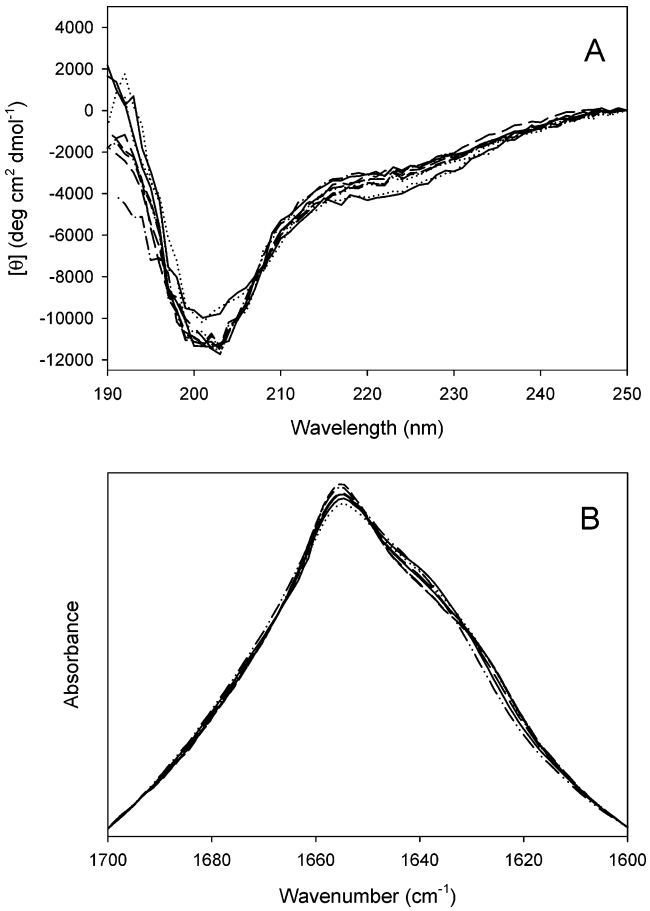

FIGURE 5: Secondary structure analysis of oxidized WT α-synuclein and its mutants with different Met → Leu substitutions. Far-UV CD (A) and FTIR spectra of the amide I region (B) were measured at pH 7.5. For the far-UV CD measurements the cell path length was 0.1 mm. Measurements were carried out at 23 °C. The protein concentration was 0.5 mg/mL. Line codes are as in Figure 2.

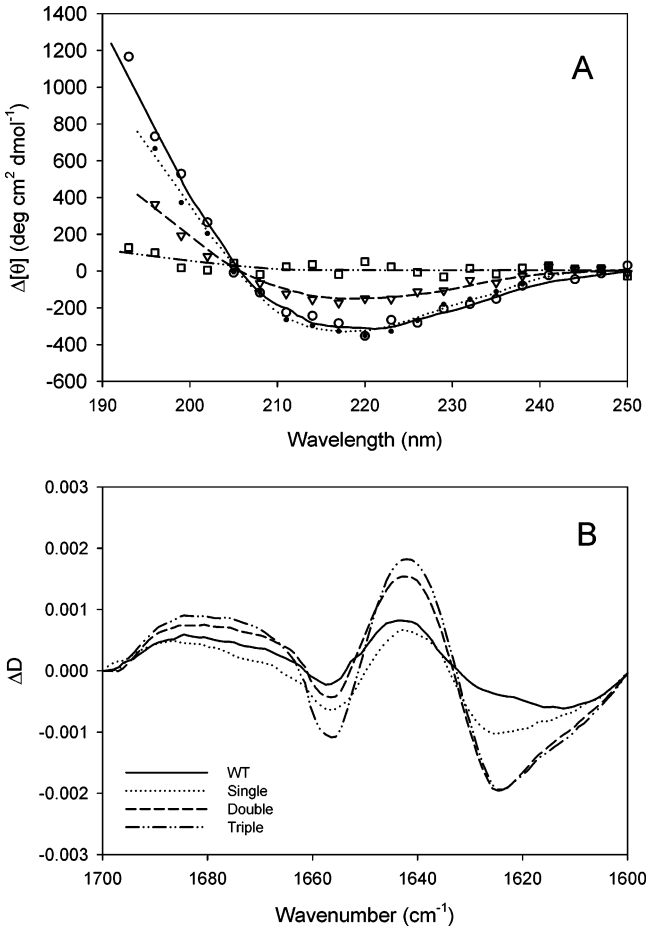

FIGURE 6: Methionine oxidation-induced changes in the secondary structure of Met → Leu variants of α-synuclein as detected by difference far-UV CD (A) and FTIR spectra (B). Difference spectra were calculated by subtraction of the spectrum for the oxidized protein from that of the corresponding nonoxidized form. These difference spectra report the excess or deficit of a particular structure in the given nonoxidized protein as compared to the corresponding oxidized protein. Symbols in plot A: WT (open circles), averaged single Met → Leu mutants (dot), averaged double Met → Leu mutants (open reversed triangles), and averaged triple Met → Leu mutants (open squares). Line codes for plot B: WT (solid), averaged single Met → Leu mutants (dotted), averaged double Met → Leu mutants (short dashes), and averaged triple Met → Leu mutants (dash-dot).

at about 208 nm. Thus, the nonoxidized proteins possess slightly more ordered structure, most likely in a form of β-structure. This means that the oxidation of α-synucleins leads to further depletion in the amount of the residual secondary structure. Interestingly, the degree of the increase in disorder was more prominent for the WT protein and its single mutants than for the double mutants, whereas the structure of the triple mutants was almost unaffected by oxidation. This clearly demonstrates a role of Met oxidation in the enhancement of disordered structure.

In agreement with the far-UV CD data, FTIR spectra also indicate some increase in the amount of disordered structure induced by oxidation (see Figure 5B). The FTIR spectra of all the α-synucleins are typical of a substantially unfolded polypeptide chain. The results of the deconvolution (FSD and second derivative) of the FTIR spectra show that MetO-α-synucleins contain smaller amounts of β-structure under

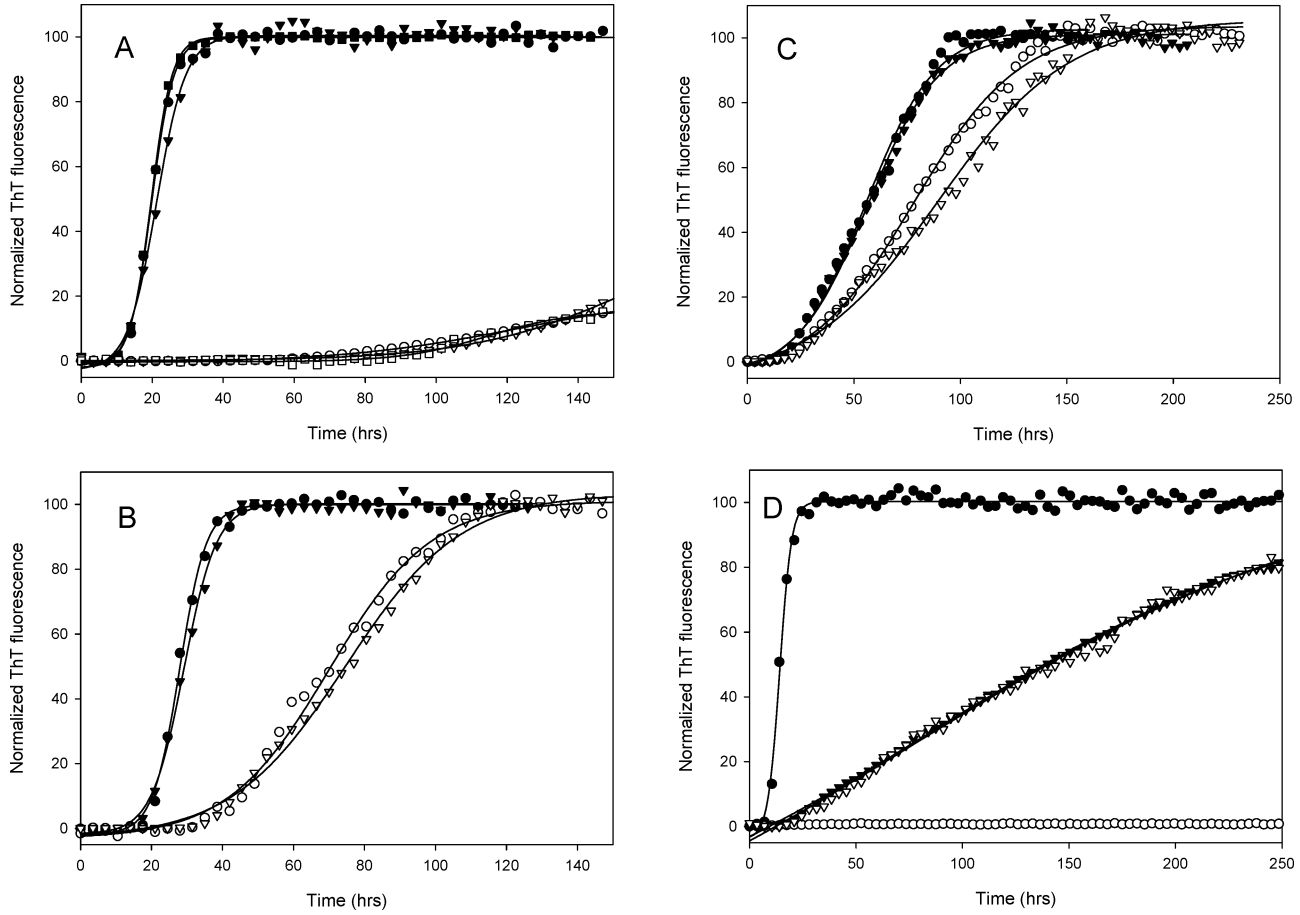

FIGURE 7: Comparison of the kinetics of fibrillation of oxidized and nonoxidized variants of α-synuclein monitored by thioflavin T fluorescence. Measurements were performed at 37 °C and pH 7.5 in 20 mM sodium phosphate buffer containing 100 mM NaCl. Panel A: M5L (circles), M116L (inverted triangles), and M127L (squares). Panel B: M5L/M127 (circles) and M116L/M127 (inverted triangles). Panel C: M5L/M116L/M127 (circles) and M116L/M127/(Met1) (inverted triangles). Panel D: WT (circles) and M5L/M116L/M127/(Met1) (inverted triangles). Black and open symbols correspond to nonmodified and MetO proteins, respectively.

these conditions. These observations are further illustrated by Figure 6B, which represents the difference FTIR spectra calculated for each protein as a difference between spectra of its nonoxidized and oxidized forms. Figure 6B shows that Met oxidation leads to a decreased signal in the vicinity of 1655 cm^{-1} (disordered conformation), occurring simultaneously with an increase around 1640 cm^{-1} (β-sheet). Thus oxidation of the methionines to the sulfoxide reduces the amount of β-structure.

The oxidation of methionine to the sulfoxide results in substitution of the hydrophobic and flexible side chain of methionine with a larger, more polar and less flexible side chain (*55*). The increased degree of unfolding of the oxidized proteins is attributed to the decreased hydrophobicity of oxidized methionine (*35*, *46*). Interestingly, another member of the synuclein family, β-synuclein, which lacks 11 residues of the central, relatively hydrophobic region of α-synuclein, also has an increased amount of disorder in comparison with α-synuclein (*56*). Thus, a decrease in the overall hydrophobicity in both β-synuclein and MetO-α-synucleins leads to a more disordered conformation, compared to α-synuclein.

Effect of Methionine Oxidation on the Fibrillation of α-Synuclein and Its Met → Leu Mutants. The rates of fibrillation of nonoxidized and oxidized α-synucleins monitored by ThT fluorescence are compared in Figure 7. The data for the mutants with three Met residues, M5L, M116L, and M127L, are summarized in Figure 7A and show that Met oxidation leads to substantially slower kinetics of fibrillation. The fibrillation kinetics of the mutants with two Mets (M5L/M127L and M116L/M127L) and one Met [M5L/M116L/M127L and M116L/M127L/(Met1)] are shown in panels B and C of Figure 7, respectively, and similarly show that the oxidized forms fibrillate more slowly than the nonoxidized forms. Figure 7D compares the fibrillation behavior of the oxidized and nonoxidized forms of the WT and the Met-minus mutant, M5L/M116L/M127L/(Met1), and shows, as expected, that there is no difference in the rate of fibrillation for the mutant lacking Met, before and after oxidation. The kinetics of fibril formation for nonoxidized WT α-synuclein at neutral pH is characterized by a typical sigmoidal curve; in contrast, there was no evidence of fibril formation by MetO-α-synuclein at neutral pH on the time scale shown (Figure 7D). In fact, fibrils were not formed even after incubation of MetO-WT for 500 h. Thus, these data confirm our previous observation that methionine oxidation inhibits fibrillation of α-synuclein at pH 7.5 (*46*).

The data in Figures 7 and 8 support the idea that the inhibitory effect on fibrillation due to methionine sulfoxide formation is uniformly distributed between the four methionines. Figure 7A shows that, in contrast to the WT protein, the oxidation of α-synucleins bearing a single Met → Leu substitution (M5L, M116L, or M127L), i.e., three Met residues, does not completely inhibit fibrillation. However, there is a considerable difference between the beginning

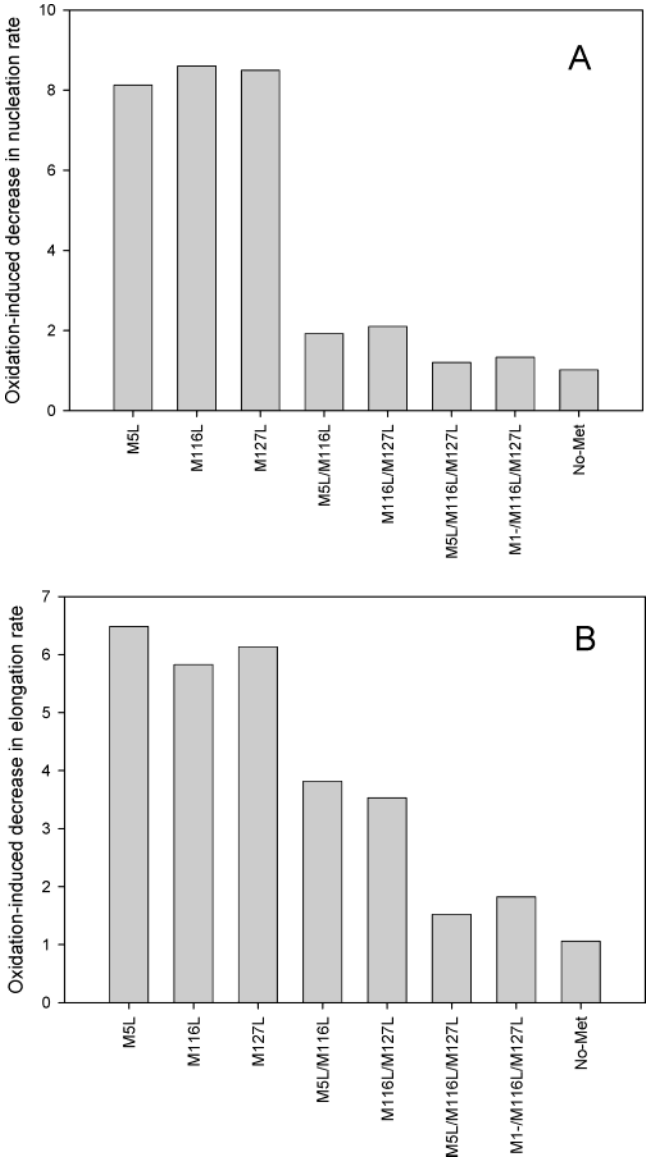

FIGURE 8: Effect of methionine oxidation on nucleation (A) and elongation rates (B) of fibrillation of α-synuclein variants with different Met → Leu substitutions. Units are per hour.

of fibrillation of the nonoxidized and MetO forms of single Met mutants (see Figure 7A and Table 2). This difference between the kinetics of fibrillation of the oxidized and nonoxidized forms decreases as the number of methionines decreases. The potential differential effects of Met oxidation on the rate of nucleation and fibril extension are examined in Figure 8. Comparison of the oxidation-induced decrease in the nucleation (A) and elongation (B) rates of human α-synuclein bearing different Met → Leu substitutions clearly shows that the oxidation of individual methionines has a cumulative effect on the fibrillation.

Effect of Metal Binding on the Fibrillation of Oxidized Forms of α-Synuclein and Its Met → Leu Mutants. Previously, we have established that the presence of metals induced partial folding of both methionine-oxidized and nonoxidized forms of WT α-synuclein. Although the fibrillation of α-synuclein at neutral pH was completely inhibited by methionine oxidation, the presence of certain metals (Ti^{3+}, Zn^{2+}, Al^{3+}, and Pb^{2+}) overcame this inhibition (*57*). We proposed that this metal ion-induced acceleration of fibrillation may be due to the relatively strong coordination of the zinc (and other metal) ion between (at least) two methionine sulfoxides. This bridging was assumed to aid the protein in adopting a necessary conformation for fibrillation, or possibly to involve intermolecular cross-bridging, which could facilitate association and subsequent fibrillation (*57*). To verify the validity of this assumption, we have analyzed the effect of zinc on the fibrillation of oxidized α-synucleins with single, double, and triple Met → Leu substitutions.

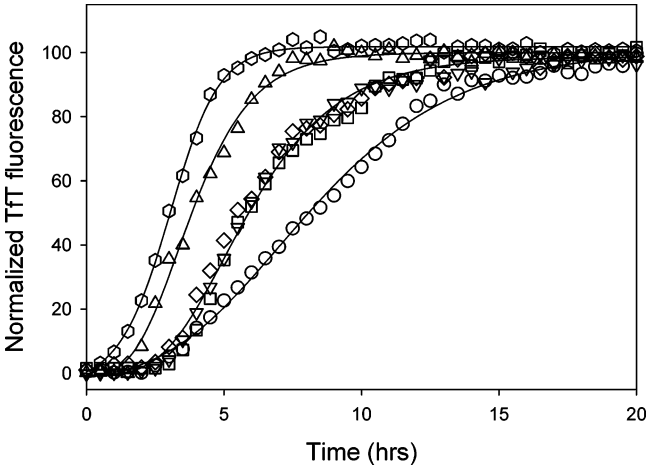

FIGURE 9: Comparison of the kinetics of fibrillation of oxidized variants of α-synuclein in the presence of 500 μM $ZnSO_4$ monitored by thioflavin T fluorescence. Measurements were performed at 37 °C and pH 7.5 in 20 mM sodium phosphate buffer containing 100 mM NaCl. Symbols: WT (circles), M5L (inverted triangles), M116L (squares), M127L (diamonds), M116L/M127 (triangles), and M5L/M116L/M127 (diamonds).

Figure 9 compares the fibrillation of the oxidized form of WT and its Met-minus mutants, M5L, M116L, M127L, M116L/M127L, and M5L/M116L/M127L, in the presence of 500 μM $ZnSO_4$. The presence of Zn^{2+} induces a dramatic acceleration of fibril formation for all of the oxidized proteins studied and in a mutation-dependent manner. In fact, all of the oxidized mutants fibrillate faster than nonmodified wild-type protein. Furthermore, the efficiency of mutation-induced acceleration of fibrillation seems to be proportional to the amount of substituted methionines, since the rates of fibrillation for the oxidized α-synucleins in the presence of Zn^{2+} can be arranged in the following order (from faster to slower rates of fibrillation): M5L/M116L/M127 > M116L/M127L > M5L ≈ M116L ≈ M127L.

These observations suggest that methionine sulfoxides of the oxidized α-synuclein are not directly involved in the coordination of Zn^{2+}, as was assumed (*57*). For example, a mutant with triple Met → Leu substitutions fibrillates faster than WT protein but would be expected to fibrillate slower or not at all if the methionine sulfoxides were involved in strong intermolecular metal interactions. In fact, interaction with Zn^{2+} seems to decrease the propensity of the Leu-substituted α-synucleins to oligomerize.

EM Analysis of Fibrils Formed by WT α-Synuclein and Its Met → Leu Mutants Shows Similar Morphology. The morphology of the fibrillar material formed by the WT α-synuclein and its Met → Leu mutants was analyzed by transmission electron microscopy. Figure 10 shows that all α-synucleins studied formed typical amyloid fibrils. The morphology of fibrils was not generally affected by the amino

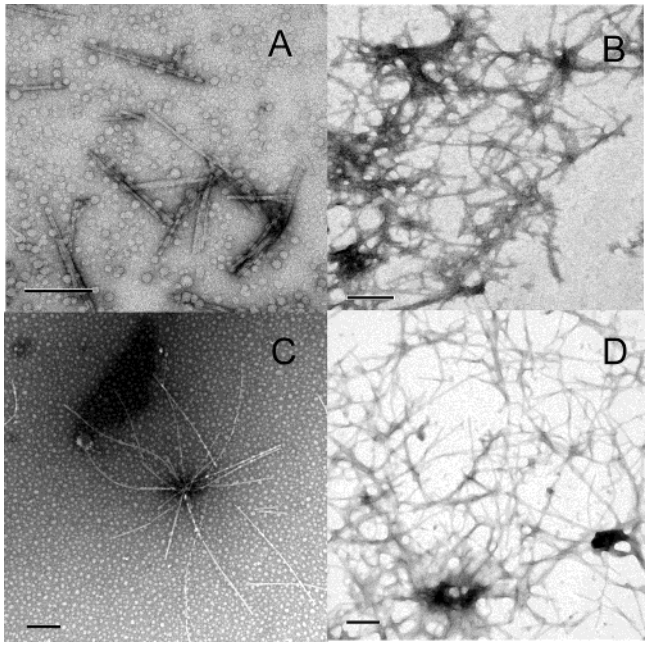

FIGURE 10: Negatively stained transmission electron micrographs of fibrils of representative nonoxidized and oxidized α-synuclein variants. Panel A: M5L. Panel B: oxidized M5L. Panel C: oxidized M5L/M116L/M127L. Panel D: M5L/M116L/M127L/(Met1). Scale bars are 200 nm.

acid substitutions or by the oxidation of the remaining methionines. In fact, all fibrils analyzed have characteristic rodlike shape, 10 ± 2 nm wide and 0.2−2 μm long.

DISCUSSION

Effect of Met → Leu Substitutions on the Structure and Fibrillation of Human α-Synuclein. Our data indicate that WT and α-synucleins with one or two Met → Leu substitutions possess similar structural properties and are typical natively unfolded proteins. On the other hand, substitutions of three Met residues by Leu lead to a very small increase in the amount of ordered secondary structure. Furthermore, in comparison to WT, all of the mutants showed increased propensity to self-associate in the order WT < three Mets < two Mets < one Met < no Met. Aggregation or self-association is known to induce additional structure in partially folded proteins (*58*, *59*), frequently in the form of increased β-structure (*49*, *51*, *60*). On the basis of these observations we attribute the changes detected in the far-UV CD and FTIR spectra to self-association. Thus, although the monomeric forms of WT and mutant α-synucleins may have very similar structural properties, our data show that the tendency of α-synuclein to associate is strongly enhanced by Met → Leu substitutions. This raises the issue of how point mutations affect the propensity to aggregate of natively unfolded proteins.

To answer this question, we compared the amino acid sequences of WT and its quadruple mutant, M5L/M116L/M127L/(Met1), which lacks Met, in terms of hydrophobicity and propensity to form β-sheet. The hydrophobicity of the mutant is obviously increased in the vicinity of each of the Met → Leu substitutions due to the larger hydrophobicity of Leu in comparison with Met [e.g., the relative hydrophobicities of Leu and Met in the normalized Kyte and Doolittle scale (*61*) are 0.92 and 0.71, respectively]. This confirms the importance of hydrophobic interactions for aggregation. Similarly, the mutant lacking methionines is more predisposed to form β-structure than WT α-synuclein as the β-sheet potential of Leu is known to be greater than that of Met (*49*). The aggregated species of many proteins are enriched in β-structure, and transformation of non-β-structure to β-structure is well-known in aggregation and fibrillation (*62*−*69*). Taking these observations into account, we hypothesize that the increased susceptibility of Met → Leu mutants to form β-sheets may not be strong enough to alter the secondary structure of the variants in their dilute monomeric state but may affect their aggregation behavior through specific stabilization of intermolecular β-structure. Furthermore, the Met → Leu substitution-induced increase in the hydrophobicity of α-synuclein also works in favor of aggregation.

Interestingly, all of the Met → Leu mutants formed fibrils more slowly than WT α-synuclein, with the number of methionines being proportional to the rate of fibril formation; with more Met residues correlating with faster fibrillation, the α-synucleins can be arranged in the following order on the basis of their rates of fibrillation, from faster to slower rates of fibrillation: WT > three Mets > two Mets > one Met > no Met. The decrease in rate of fibrillation, induced by the Met → Leu substitutions, correlates with the increased propensity of the mutated α-synucleins to oligomerize (see above). This indicates that the mutants form oligomers that are not on the productive pathway of fibril assembly.

Effect of Methionine Oxidation on the Structure and Fibrillation of WT and Mutant Forms of α-Synuclein. Previously, we demonstrated that in vitro hydrogen peroxide readily oxidizes the four methionines in α-synuclein to their corresponding sulfoxides. This modification was shown to inhibit the fibrillation of α-synuclein (*46*). Here we show that the degree of inhibition of fibrillation by MetO α-synuclein is proportional to the number of oxidized methionines and that the fibrillation kinetics of α-synucleins with one oxidized Met were relatively similar to those of the corresponding nonoxidized proteins. For the double α-synuclein mutants with two methionines, the oxidized forms formed fibrils substantially more slowly, and for the mutants with three oxidized Met residues, the kinetics were dramatically slower.

There is a somewhat greater effect of methionine oxidation on the lag time for fibrillation, compared to fibril growth, but the fibrillation kinetics in general were very similar for each variant with the same number of methionine sulfoxides. Thus, we conclude that the oxidation of individual methionines contributes to a similar degree to the inhibition of MetO α-synuclein fibrillation and that there are no significant sequence-specific effects. The decreased rate of fibrillation with increasing numbers of oxidized Mets is attributed to the decrease in α-synuclein residual structure.

Data on the effect of metal binding on fibrillation of oxidized WT α-synuclein and its methionine mutants help to further illuminate the role of Met → Leu substitution in the fibrillation process. As noted, in the presence of Zn^{2+} all of the oxidized mutants fibrillate faster than WT protein, with the mutation-induced acceleration of fibrillation proportional to the number of leucine residues (one Met, three new Leu > two Met, two new Leu > three Met, one new Leu > WT, no new Leu). This observation indicates that

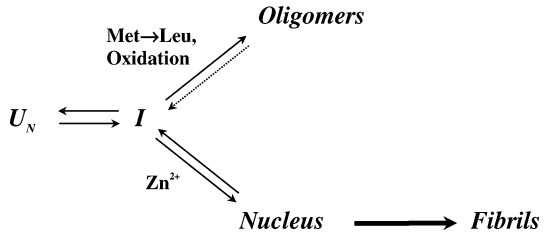

FIGURE 11: Model for the fibrillation of WT and Met → Leu substituted α-synucleins and fibrillation of methionine-oxidized α-synucleins in the presence of Zn^{2+}. The presence of Leu residues in place of Met and/or Met oxidation lead(s) to preferential partitioning to populate stable soluble oligomers, whereas the presence of Zn^{2+} with either oxidized or nonoxidized α-synuclein leads to partitioning in favor of fibrils (see text).

the oxidized methionines are not directly involved in the coordination of Zn^{2+}. Furthermore, metal binding and methionine substitution/oxidation affect different parts of the protein and modulate aggregation of α-synuclein via different mechanisms. We assume that Zn^{2+} binding is the prevalent amyloidogenic factor, whereas methionine substitution/oxidation plays a secondary and mostly regulatory role in this process.

A model for the aggregation of α-synuclein is shown in Figure 11. In the model, I represents a partially folded conformation, which undergoes kinetic partitioning between pathways leading to fibrils or soluble oligomers (and potentially amorphous aggregates). The fibrillation of WT α-synuclein is believed to occur via a nucleation-dependent polymerization mechanism (*17*, *20*), with a critical initial structural transformation from the unfolded conformation to a partially folded species (*4*). The WT protein can also form soluble off-pathway oligomers, but the population is low under typical fibrillation conditions. On the basis of the observations in the current study, we propose that the Met → Leu substitutions lead to a shift in the partitioning of the partially folded intermediate in favor of the soluble oligomers. There are two explanations for this: either the structure of the intermediate is different, due to the increased hydrophobicity of the Leu residues, or the stability (and perhaps the structure) of the oligomers is different from that observed for the WT protein. Similarly, we assume that methionine oxidation also favors partitioning to the soluble oligomers, probably by substantially stabilizing them.

The effectiveness of Zn^{2+} in accelerating fibrillation of both oxidized WT and mutated α-synucleins indicates that the presence of Zn^{2+} causes partitioning in favor of the fibrillation pathway. Thus, Zn^{2+} overcomes the factors that lead to population and stabilization of the soluble oligomers.

Overall, our data suggest that the entire chain, or at least the N- and C-terminal regions that contain the methionines, is directly involved in the self-association and fibril formation. It is interesting to compare these findings with what is currently known about involvement of different α-synuclein fragments in fibril formation. First of all, analysis of literature data implicates the crucial amyloidogenic role of the central hydrophobic region, known as the NAC peptide (residues 61−95). NAC is a major component of amyloid plaques in Alzheimer's brain (*70*) and readily forms ordered fibrils in vitro (*2*, *70*, *71*). Furthermore, although β-synuclein is highly homologous to α-synuclein, it does not fibrillate due to the lack of an 11 amino acid segment within the central part of the NAC domain (corresponding to residues 73−83 of α-synuclein) (*72*−*74*). The substitution of Ala76 with charged amino acids (either Arg or Glu) decreases the rate of α-synuclein association (*75*), whereas the deletion of amino acid residues 71−82 in human α-synuclein prevents protein aggregation (*75*). Interestingly, it has been shown that the amyloidogenicity is not uniformly distributed even within NAC (*75*−*79*).

The characteristic feature of the amino acid sequence of the α-synuclein N-terminus is seven 11 amino acid repeats (XKTKEGVXXXX) (*1*), which can form an amphipathic α-helix typical of the lipid-binding motif of apolipoproteins (*80*, *81*). It has been shown recently that a variant of α-synuclein with two additional repeats disfavors the formation of β-sheet-rich oligomers, including amyloid fibrils. In contrast, a truncated variant with two fewer repeats favors β-sheet and fibril formation (*82*). On the basis of these observations it has been proposed that the number of repeats in α-synuclein represents an evolutionary balance between the functional conformer of α-synuclein (α-helix and/or random coil) and its pathogenic β-sheet conformation and that the N-terminal truncation of α-synuclein may promote pathogenesis (*82*). Comparison of the fibrillation and aggregation rates of WT with those of the familial PD mutations, A30P and A53T, revealed the N-terminal domain of human α-synuclein as another part of the molecule that plays an important role in the modulation of aggregation and fibrillation. It has been shown that both these familial PD mutations increase the rate of α-synuclein oligomerization, whereas the rate of mature fibril formation was increased by one (A53T) and decreased by the other (A30P) (*16*, *17*, *49*, *83*−*85*). These observations are in a good agreement with the results of the WT, A30P, and A53T amino acid sequence analysis in terms of propensity to form β-sheet structure (*49*).

The C-terminal region of α-synuclein, residues 96−149, is enriched in acidic residues and prolines, indicating that it adopts a disordered conformation. It has been suggested that the charge and hydrophobicity distribution within the C-terminal domain may play a role in the regulation of α-synuclein aggregation (*86*). In fact, it has been shown that C-terminally truncated human α-synucleins (1−130, 1−120, and 1−110) assembled into fibrils much more readily than the full-length protein (*18*). Furthermore, the C-terminal domain of γ-synuclein, a protein which was shown to form soluble oligomers most readily among the members of synuclein family (*73*), has the smallest net charge (−4), whereas the carboxy-terminal part of nonamyloidogenic β-synuclein has the largest net charge (−16).

The data presented above emphasize that all parts of α-synuclein are important for its aggregation. Our finding that methionine oxidation plays an important role in inhibiting α-synuclein aggregation is in agreement with this idea. Interestingly, all of the methionines are located outside the NAC region, and none of them is a part of a repeat sequence of α-synuclein. The methionines are in very different surroundings, with Met116 and Met127 being located in the very polar C-terminal region, whereas Met1 and Met5 are in a more hydrophobic local environment. The precise molecular mechanism of how oxidation of methionines inhibits the fibrillation of human α-synuclein is unclear as yet, although it must involve preferential formation and stabilization of soluble oligomers. However, some hints can

be obtained from analysis of recent solution NMR studies on the effect of methionine oxidation on structure of Aβ(1−40) and Aβ(1−42), natively unfolded peptides involved into the pathogenesis of Alzheimer's disease via the aggregation and formation specific amyloid plaques (*87*). Earlier it has been shown that, analogous to α-synuclein, oxidation of the single Met35 to the sulfoxide significantly impedes the rate of fibrillation of the Aβ peptide (*88*). NMR analysis revealed that the oxidized and nonoxidized forms of Aβ(1−40) and Aβ(1−42) peptides are largely random, extended chain structures, with the oxidation of Met35 reducing the propensity for β-strand structure at two hydrophobic regions (Leu17−Ala21 and Ile31−Val36) and turn- or bend-like structures at Asp7−Glu11 and Phe20−Ser26. The NMR data indicated that the oxidation of Met35 significantly hindered the movements of the His6, His13, and His14 side chains. On the basis of these observations it has been concluded that the oxidation of single Met35 prevents aggregation by reducing both hydrophobic and electrostatic association (*89*). These NMR data also emphasized that oxidation may affect residual structure in unfolded Aβ(1−40) and Aβ(1−42) peptides in close proximity to Met35 and modify structure and interactions of polypeptide parts distant from this residue. A similar situation may occur in α-synuclein.

REFERENCES

1. Maroteaux, L., Campanelli, J. T., and Scheller, R. H. (1988) Synuclein: a neuron-specific protein localized to the nucleus and presynaptic nerve terminal, *J. Neurosci. 8*, 2804−2815.
2. Iwai, A., Masliah, E., Yoshimoto, M., Ge, N., Flanagan, L., de Silva, H. A., Kittel, A., and Saitoh, T. (1995) The precursor protein of non-A beta component of Alzheimer's disease amyloid is a presynaptic protein of the central nervous system, *Neuron 14*, 467−475.
3. Weinreb, P. H., Zhen, W. G., Poon, A. W., Conway, K. A., and Lansbury, P. T., Jr. (1996) NACP, a protein implicated in Alzheimer's disease and learning, is natively unfolded, *Biochemistry 35*, 13709−13715.
4. Uversky, V. N., Li, J., and Fink, A. L. (2001) Evidence for a partially folded intermediate in alpha-synuclein fibril formation, *J. Biol. Chem. 276*, 10737−10744.
5. Uversky, V. N., Gillespie, J. R., and Fink, A. L. (2000) Why are "natively unfolded" proteins unstructured under physiologic conditions?, *Proteins 41*, 415−427.
6. Goedert, M. (2001) Parkinson's disease and other alpha-synucleinopathies, *Clin. Chem. Lab. Med. 39*, 308−312.
7. Trojanowski, J. Q., and Lee, V. M. (2003) Parkinson's disease and related alpha-synucleinopathies are brain amyloidoses, *Ann. N.Y. Acad. Sci. 991*, 107−110.
8. Spillantini, M. G., Schmidt, M. L., Lee, V. M., Trojanowski, J. Q., Jakes, R., and Goedert, M. (1997) Alpha-synuclein in Lewy bodies, *Nature 388*, 839−840.
9. Lewy, F. H. (1912) in *Handbuch der Neurologie* (Lewandowski, M., Ed.) pp 920−933, Springer, Berlin.
10. Forno, L. S. (1996) Neuropathology of Parkinson's disease, *J. Neuropathol. Exp. Neurol. 55*, 259−272.
11. Polymeropoulos, M. H., Lavedan, C., Leroy, E., Ide, S. E., Dehejia, A., Dutra, A., Pike, B., Root, H., Rubenstein, J., Boyer, R., Stenroos, E. S., Chandrasekharappa, S., Athanassiadou, A., Papapetropoulos, T., Johnson, W. G., Lazzarini, A. M., Duvoisin, R. C., Di Iorio, G., Golbe, L. I., and Nussbaum, R. L. (1997) Mutation in the alpha-synuclein gene identified in families with Parkinson's disease, *Science 276*, 2045−2047.
12. Kruger, R., Kuhn, W., Muller, T., Woitalla, D., Graeber, M., Kosel, S., Przuntek, H., Epplen, J. T., Schols, L., and Riess, O. (1998) Ala30Pro mutation in the gene encoding alpha-synuclein in Parkinson's disease, *Nat. Genet. 18*, 106−108.
13. Singleton, A. B., Farrer, M., Johnson, J., Singleton, A., Hague, S., Kachergus, J., Hulihan, M., Peuralinna, T., Dutra, A., Nussbaum, R., Lincoln, S., Crawley, A., Hanson, M., Maraganore, D., Adler, C., Cookson, M. R., Muenter, M., Baptista, M., Miller, D., Blancato, J., Hardy, J., and Gwinn-Hardy, K. (2003) alpha-Synuclein locus triplication causes Parkinson's disease, *Science 302*, 841.
14. Masliah, E., Rockenstein, E., Veinbergs, I., Mallory, M., Hashimoto, M., Takeda, A., Sagara, Y., Sisk, A., and Mucke, L. (2000) Dopaminergic loss and inclusion body formation in alpha-synuclein mice: implications for neurodegenerative disorders, *Science 287*, 1265−1269.
15. Feany, M. B., and Bender, W. W. (2000) A Drosophila model of Parkinson's disease, *Nature 404*, 394−398.
16. Conway, K. A., Harper, J. D., and Lansbury, P. T. (1998) Accelerated in vitro fibril formation by a mutant alpha-synuclein linked to early-onset Parkinson disease, *Nat. Med. 4*, 1318−1320.
17. Conway, K. A., Lee, S. J., Rochet, J. C., Ding, T. T., Williamson, R. E., and Lansbury, P. T., Jr. (2000) Acceleration of oligomerization, not fibrillization, is a shared property of both alpha-synuclein mutations linked to early-onset Parkinson's disease: implications for pathogenesis and therapy, *Proc. Natl. Acad. Sci. U.S.A. 97*, 571−576.
18. Crowther, R. A., Jakes, R., Spillantini, M. G., and Goedert, M. (1998) Synthetic filaments assembled from C-terminally truncated alpha-synuclein, *FEBS Lett. 436*, 309−312.
19. Giasson, B. I., Uryu, K., Trojanowski, J. Q., and Lee, V. M. Y. (1999) Mutant and wild-type human alpha-synuclein assemble into elongated filaments with distinct morphologies in vitro, *J. Biol. Chem. 274*, 7619−7622.
20. Wood, S. J., Wypych, J., Steavenson, S., Louis, J. C., Citron, M., and Biere, A. L. (1999) Alpha-synuclein fibrillogenesis is nucleation-dependent, *J. Biol. Chem. 274*, 19509−19512.
21. Serpell, L. C., Berriman, J., Jakes, R., Goedert, M., and Crowther, R. A. (2000) Fiber diffraction of synthetic alpha-synuclein filaments shows amyloid-like cross-beta conformation, *Proc. Natl. Acad. Sci. U.S.A. 97*, 4897−4902.
22. Stadtman, E. R., Oliver, C. N., Starke-Reed, P. E., and Rhee, S. G. (1993) Age-related oxidation reaction in proteins, *Toxicol. Ind. Health 9*, 187−196.
23. Stadtman, E. R., and Berlett, B. S. (1997) Reactive oxygen-mediated protein oxidation in aging and disease, *Chem. Res. Toxicol. 10*, 485−494.
24. Leeuwenburgh, C., Hansen, P., Shaish, A., Holloszy, J. O., and Heinecke, J. W. (1998) Markers of protein oxidation by hydroxyl radical and reactive nitrogen species in tissues of aging rats, *Am. J. Physiol. 43*, R453−R461.
25. Butterfield, D. A., Howard, B., Yatin, S., Koppal, T., Drake, J., Hensley, K., Aksenov, M., Aksenova, M., Subramaniam, R., Varadarajan, S., Harris-White, M. E., Pedigo, N. W., Jr., and Carney, J. M. (1999) Elevated oxidative stress in models of normal brain aging and Alzheimer's disease, *Life Sci. 65*, 1883−1892.
26. Smith, C. D., Carney, J. M., Starke-Reed, P. E., Oliver, C. N., Stadtman, E. R., Floyd, R. A., and Markesbery, W. R. (1991) Excess brain protein oxidation and enzyme dysfunction in normal aging and in Alzheimer disease, *Proc. Natl. Acad. Sci U.S.A. 88*, 10540−10543.
27. Aksenova, M. V., Aksenov, M. Y., Payne, R. M., Trojanowski, J. Q., Schmidt, M. L., Carney, J. M., Butterfield, D. A., and Markesbery, W. R. (1999) Oxidation of cytosolic proteins and expression of creatine kinase BB in frontal lobe in different neurodegenerative disorders, *Dementia Geriatr. Cognit. Disord. 10*, 158−165.
28. Markesbery, W. R., and Carney, J. M. (1999) Oxidative alterations in Alzheimer's disease, *Brain Pathol. 9*, 133−146.
29. Duda, J. E., Giasson, B. I., Chen, Q., Gur, T. L., Hurtig, H. I., Stern, M. B., Gollomp, S. M., Ischiropoulos, H., Lee, V. M., and Trojanowski, J. Q. (2000) Widespread nitration of pathological inclusions in neurodegenerative synucleinopathies, *Am. J. Pathol. 157*, 1439−1445.
30. Jenner, P., Dexter, D. T., Sian, J., Schapira, A. H., and Marsden, C. D. (1992) Oxidative stress as a cause of nigral cell death in Parkinson's disease and incidental Lewy body disease. The Royal Kings and Queens Parkinson's Disease Research Group, *Ann. Neurol. 32* (Suppl.), S82−S87.
31. Jenner, P. (2003) Oxidative stress in Parkinson's disease, *Ann. Neurol. 53* (Suppl. 3), S26−S36.
32. Lyras, L., Perry, R. H., Perry, E. K., Ince, P. G., Jenner, A., Jenner, P., and Halliwell, B. (1998) Oxidative damage to proteins, lipids, and DNA in cortical brain regions from patients with dementia with Lewy bodies, *J. Neurochem. 71*, 302−312.

33. Browne, S. E., Ferrante, R. J., and Beal, M. F. (1999) Oxidative stress in Huntington's disease, *Brain Pathol. 9*, 147−163.
34. Cookson, M. R., and Shaw, P. J. (1999) Oxidative stress and motor neurone disease, *Brain Pathol. 9*, 165−186.
35. Vogt, W. (1995) Oxidation of methionyl residues in proteins: tools, targets, and reversal, *Free Radical Biol. Med. 18*, 93−105.
36. Moskovitz, J., Weissbach, H., and Brot, N. (1996) Cloning the expression of a mammalian gene involved in the reduction of methionine sulfoxide residues in proteins, *Proc. Natl. Acad. Sci. U.S.A. 93*, 2095−2099.
37. Sun, H., Gao, J., Ferrington, D. A., Biesiada, H., Williams, T. D., and Squier, T. C. (1999) Repair of oxidized calmodulin by methionine sulfoxide reductase restores ability to activate the plasma membrane Ca-ATPase, *Biochemistry 38*, 105−112.
38. Levine, R. L., Mosoni, L., Berlett, B. S., and Stadtman, E. R. (1996) Methionine residues as endogenous antioxidants in proteins, *Proc. Natl. Acad. Sci. U.S.A. 93*, 15036−15040.
39. Uversky, V. N., Li, J., Bower, K., and Fink, A. L. (2002) Synergistic effects of pesticides and metals on the fibrillation of alpha-synuclein: Implications for Parkinson's disease, *Neurotoxicology 23*, 527−536.
40. Uversky, V. N., and Fink, A. L. (2002) Biophysical properties of human alpha-synuclein and its role in Parkinson's disease, in *Recent Research Developments in Proteins* (Pandalai, S. G., Ed.) pp 153−186, Transworld Research Network, Kerala, India.
41. Yoritaka, A., Hattori, N., Uchida, K., Tanaka, M., Stadtman, E. R., and Mizuno, Y. (1996) Immunohistochemical detection of 4-hydroxynonenal protein adducts in Parkinson disease, *Proc. Natl. Acad. Sci. U.S.A. 93*, 2696−2701.
42. Good, P. F., Hsu, A., Werner, P., Perl, D. P., and Olanow, C. W. (1998) Protein nitration in Parkinson's disease, *J Neuropathol. Exp. Neurol. 57*, 338−342.
43. Giasson, B. I., Duda, J. E., Murray, I. V., Chen, Q., Souza, J. M., Hurtig, H. I., Ischiropoulos, H., Trojanowski, J. Q., and Lee, V. M. (2000) Oxidative damage linked to neurodegeneration by selective alpha- synuclein nitration in synucleinopathy lesions, *Science 290*, 985−989.
44. Paik, S. R., Shin, H. J., and Lee, J. H. (2000) Metal-catalyzed oxidation of alpha-synuclein in the presence of copper(II) and hydrogen peroxide, *Arch. Biochem. Biophys. 378*, 269−277.
45. Conway, K. A., Rochet, J. C., Bieganski, R. M., and Lansbury, P. T., Jr. (2001) Kinetic stabilization of the alpha-synuclein protofibril by a dopamine-alpha-synuclein adduct, *Science 294*, 1346−1349.
46. Uversky, V. N., Yamin, G., Souillac, P. O., Goers, J., Glaser, C. B., and Fink, A. L. (2002) Methionine oxidation inhibits fibrillation of human alpha-synuclein in vitro, *FEBS Lett. 517*, 239−244.
47. Oberg, K. A., and Fink, A. L. (1998) A new attenuated total reflectance Fourier transform infrared spectroscopy method for the study of proteins in solution, *Anal. Biochem. 256*, 92−106.
48. Nielsen, L., Khurana, R., Coats, A., Frokjaer, S., Brange, J., Vyas, S., Uversky, V. N., and Fink, A. L. (2001) Effect of environmental factors on the kinetics of insulin fibril formation: Elucidation of the molecular mechanism, *Biochemistry 40*, 6036−6046.
49. Li, J., Uversky, V. N., and Fink, A. L. (2001) Effect of familial Parkinson's disease point mutations A30P and A53T on the structural properties, aggregation, and fibrillation of human alpha-synuclein, *Biochemistry 40*, 11604−11613.
50. Uversky, V. N., Li, J., Souillac, P., Jakes, R., Goedert, M., and Fink, A. L. (2002) Biophysical properties of the synucleins and their propensities to fibrillate: inhibition of alpha-synuclein assembly by beta- and gamma-synucleins, *J. Biol. Chem. 277*, 11970−11978.
51. Munishkina, L. A., Phelan, C., Uversky, V. N., and Fink, A. L. (2003) Conformational behavior and aggregation of alpha-synuclein in organic solvents: Modeling the effects of membranes, *Biochemistry 42*, 2720−2730.
52. Naiki, H., Higuchi, K., Matsushima, K., Shimada, A., Chen, W. H., Hosokawa, M., and Takeda, T. (1990) Fluorometric examination of tissue amyloid fibrils in murine senile amyloidosis: use of the fluorescent indicator, thioflavine T, *Lab. Invest. 62*, 768−773.
53. Naiki, H., Higuchi, K., Hosokawa, M., and Takeda, T. (1989) Fluorometric determination of amyloid fibrils in vitro using the fluorescent dye, thioflavin T, *Anal. Biochem. 177*, 244−249.
54. Naiki, H., Higuchi, K., Nakakuki, K., and Takeda, T. (1991) Kinetic analysis of amyloid fibril polymerization in vitro, *Lab. Invest. 65*, 104−110.
55. Kim, Y. H., Berry, A. H., Spencer, D. S., and Stites, W. E. (2001) Comparing the effect on protein stability of methionine oxidation versus mutagenesis: steps toward engineering oxidative resistance in proteins, *Protein Eng. 14*, 343−347.
56. Uversky, V. N., Li, J., Souillac, P., Jakes, R., Goedert, M., and Fink, A. L. (2002) Biophysical properties of the synucleins and their propensities to fibrillate: inhibition of alpha-synuclein assembly by beta- and gamma-synucleins, *J. Biol. Chem. 277*, 11970−11978.
57. Yamin, G., Glaser, C. B., Uversky, V. N., and Fink, A. L. (2003) Certain metals trigger fibrillation of methionine-oxidized alpha-synuclein, *J. Biol. Chem 278*, 27630−27635.
58. Uversky, V. N., Karnoup, A. S., Khurana, R., Segel, D. J., Doniach, S., and Fink, A. L. (1999) Association of partially folded intermediates of staphylococcal nuclease induces structure and stability, *Protein Sci. 8*, 161−173.
59. Kuznetsova, I. M., Biktashev, A. G., Khaitlina, S. Y., Vassilenko, K. S., Turoverov, K. K., and Uversky, V. N. (1999) Effect of self-association on the structural organization of partially folded proteins: inactivated actin, *Biophys. J. 77*, 2788−2800.
60. Uversky, V. N., Li, J., Souillac, P., Jakes, R., Goedert, M., and Fink, A. L. (2002) Biophysical properties of the synucleins and their propensities to fibrillate: inhibition of alpha-synuclein assembly by beta- and gamma-synucleins, *J. Biol. Chem. 277*, 11970−11978.
61. Kyte, J., and Doolittle, R. F. (1982) A simple method for displaying the hydropathic character of a protein, *J. Mol. Biol. 157*, 105−132.
62. Fink, A. L., Seshadri, S., Khurana, R., and Oberg, K. A. (1999) in *Infrared Analysis of Peptides and Proteins* (Singh, B. R., Ed.) pp 132−144, American Chemical Society, Washington, DC.
63. Oberg, K., Chrunyk, B. A., Wetzel, R., and Fink, A. L. (1994) Nativelike secondary structure in interleukin-1 beta inclusion bodies by attenuated total reflectance FTIR, *Biochemistry 33*, 2628−2634.
64. Ismail, A. A., Mantsch, H. H., and Wong, P. T. T. (1992) Aggregation of chymotrypsinogen—portrait by infrared spectroscopy, *Biochim. Biophys. Acta 1121*, 183−188.
65. Przybycien, T. M., Dunn, J. P., Valax, P., and Georgiou, G. (1994) Secondary structure characterization of beta-lactamase inclusion bodies, *Protein Eng. 7*, 131−136.
66. Kendrick, B. S., Cleland, J. L., Lam, X., Nguyen, T., Randolph, T. W., Manning, M. C., and Carpenter, J. F. (1998) Aggregation of recombinant human interferon gamma: kinetics and structural transitions, *J. Pharm. Sci. 87*, 1069−1076.
67. Clark, A. H., Saunderson, D. H., and Suggett, A. (1981) Infrared and laser-Raman spectroscopic studies of thermally-induced globular protein gels, *Int. J. Pept. Protein Res. 17*, 353−364.
68. Fink, A. L. (1998) Protein aggregation: folding aggregates, inclusion bodies and amyloid, *Folding Des. 3*, 9−15.
69. Nielsen, L., Frokjaer, S., Carpenter, J. F., and Brange, J. (2001) Studies of the structure of insulin fibrils by Fourier transform infrared (FTIR) spectroscopy and electron microscopy, *J. Pharm. Sci. 90*, 29−37.
70. Ueda, K., Fukushima, H., Masliah, E., Xia, Y., Iwai, A., Yoshimoto, M., Otero, D. A., Kondo, J., Ihara, Y., and Saitoh, T. (1993) Molecular cloning of cDNA encoding an unrecognized component of amyloid in Alzheimer disease, *Proc. Natl. Acad. Sci. U.S.A. 90*, 11282−11286.
71. Han, H., Weinreb, P. H., and Lansbury, P. T., Jr. (1995) The core Alzheimer's peptide NAC forms amyloid fibrils which seed and are seeded by beta-amyloid: is NAC a common trigger or target in neurodegenerative disease?, *Chem. Biol. 2*, 163−169.
72. Hashimoto, M., Rockenstein, E., Mante, M., Mallory, M., and Masliah, E. (2001) beta-Synuclein inhibits alpha-synuclein aggregation. A possible role as an anti-parkinsonian factor, *Neuron 32*, 213−223.
73. Uversky, V. N., Li, J., Souillac, P., Millett, I. S., Doniach, S., Jakes, R., Goedert, M., and Fink, A. L. (2002) Biophysical properties of the synucleins and their propensities to fibrillate—Inhibition of alpha-synuclein assembly by beta- and gamma-synucleins, *J. Biol. Chem. 277*, 11970−11978.
74. Park, J. Y., and Lansbury, P. T. (2003) beta-synuclein inhibits formation of alpha-synuclein protofibrils: A possible therapeutic strategy against Parkinson's disease, *Biochemistry 42*, 3696−3700.
75. Giasson, B. I., Murray, I. V., Trojanowski, J. Q., and Lee, V. M. (2001) A hydrophobic stretch of 12 amino acid residues in the middle of alpha-synuclein is essential for filament assembly, *J. Biol. Chem. 276*, 2380−2386.

76. Bodles, A. M., Guthrie, D. J., Greer, B., and Irvine, G. B. (2001) Identification of the region of non-Abeta component (NAC) of Alzheimer's disease amyloid responsible for its aggregation and toxicity, *J. Neurochem. 78*, 384−395.
77. Bodles, A. M., Guthrie, D. J., Harriott, P., Campbell, P., and Irvine, G. B. (2000) Toxicity of non-abeta component of Alzheimer's disease amyloid, and N-terminal fragments thereof, correlates to formation of beta-sheet structure and fibrils, *Eur. J. Biochem. 267*, 2186−2194.
78. Irvine, G. B., El Agnaf, O. M., Bodles, A. M., Guthrie, D. J., and Harriott, P. (1998) Studies on the aggregation and secondary structure of peptides derived from non-A beta component of Alzheimer's disease amyloid, *Biochem. Soc. Trans. 26*, S36.
79. El Agnaf, O. M., Bodles, A. M., Guthrie, D. J., Harriott, P., and Irvine, G. B. (1998) The N-terminal region of non-A beta component of Alzheimer's disease amyloid is responsible for its tendency to assume beta-sheet and aggregate to form fibrils, *Eur. J. Biochem. 258*, 157−163.
80. Clayton, D. F., and George, J. M. (1998) The synucleins: a family of proteins involved in synaptic function, plasticity, neurodegeneration and disease, *Trends Neurosci. 21*, 249−254.
81. George, J. M., Jin, H., Woods, W. S., and Clayton, D. F. (1995) Characterization of a novel protein regulated during the critical period for song learning in the zebra finch, *Neuron 15*, 361−372.
82. Kessler, J. C., Rochet, J. C., and Lansbury, P. T. (2003) The N-terminal repeat domain of alpha-synuclein inhibits beta-sheet and amyloid fibril formation, *Biochemistry 42*, 672−678.
83. Conway, K. A., Harper, J. D., and Lansbury, P. T., Jr. (2000) Fibrils formed in vitro from alfa-synuclein and two mutant forms linked to Parkinson's disease are typical amyloid, *Biochemistry 39*, 2552−2563.
84. Narhi, L., Wood, S. J., Steavenson, S., Jiang, Y., Wu, G. M., Anafi, D., Kaufman, S. A., Martin, F., Sitney, K., Denis, P., Louis, J. C., Wypych, J., Biere, A. L., and Citron, M. (1999) Both familial Parkinson's disease mutations accelerate alpha-synuclein aggregation, *J. Biol. Chem. 274*, 9843−9846.
85. Li, J., Uversky, V. N., and Fink, A. L. (2002) Conformational behavior of human alpha-synuclein is modulated by familial Parkinson's disease point mutations A30P and A53T, *Neurotoxicology 23*, 553−567.
86. Uversky, V. N., and Fink, A. L. (2002) Amino acid determinants of alpha-synuclein aggregation: putting together pieces of the puzzle, *FEBS Lett. 522*, 9−13.
87. Trojanowski, J. Q., and Lee, V. M. (2000) "Fatal attractions" of proteins. A comprehensive hypothetical mechanism underlying Alzheimer's disease and other neurodegenerative disorders, *Ann. N.Y. Acad. Sci. 924*, 62−67.
88. Hou, L., Kang, I., Marchant, R. E., and Zagorski, M. G. (2002) Methionine 35 oxidation reduces fibril assembly of the amyloid abeta-(1−42) peptide of Alzheimer's disease, *J. Biol. Chem. 277*, 40173−40176.
89. Hou, L., Shao, H., Zhang, Y., Li, H., Menon, N. K., Neuhaus, E. B., Brewer, J. M., Byeon, I.-J. L., Ray, D. G., Vitek, M. P., Iwashita, T., Makula, R. A., Przybyla, A. B., and Zagorski, M. G. (2004) Solution NMR studies of the amyloid beta(1−40) and amyloid beta(1−42) peptides establish that the Met35 oxidation state affects the mechanism of amyloid formation, *J. Am. Chem. Soc.* (in press).

BI049979H